
GRAPH NEURAL NETWORK SURROGATE FOR SEISMIC RELIABILITY ANALYSIS OF HIGHWAY BRIDGE SYSTEM

A PREPRINT

Tong Liu

Department of Civil and Environmental Engineering
University of Illinois at Urbana-Champaign
tongl5@illinois.edu

Hadi Meidani

Department of Civil and Environmental Engineering
University of Illinois at Urbana-Champaign
meidani@illinois.edu

October 13, 2022

ABSTRACT

Rapid reliability assessment of transportation networks can enhance preparedness, risk mitigation and response management procedures related to these systems. Network reliability approaches commonly consider network-level responses, and due to computational cost do not consider the more detailed node-level responses. In this paper, we propose a rapid seismic reliability assessment approach for bridge networks based on graph neural networks, where node-level connectivities, between points of interest and other nodes, are quantified under probabilistic bridge conditions and earthquake events. Via numerical experiments on transportation systems in California, we demonstrate the accuracy, computational efficiency and robustness of the proposed approach compared to the Monte Carlo approach.

1 Introduction

Extreme hazards continue to influence the infrastructure system, with losses exceeding hundreds of billion of dollars. For instance, the overall cost to repair or replace the infrastructure system during hurricane Katrina in 2005 [1] is over \$1 billion. The cost for postdisaster reconstruction and ecological rehabilitation after Wenchuan Earthquake in 2008 is over \$100 billion [2]. The transportation system is one of the 16 critical infrastructure sectors according to Cyber Infrastructure Security Agency (CISA) [3]. The highway system in the US, for instance, encompasses over 164,000 miles in the National Highway System (NHS). The society relies on the highway system also during emergencies for access to critical facilities, including hospitals, airports, fire stations, etc. Highway bridges are critical, and yet vulnerable, components of the transportation infrastructure. The United States has a national inventory of almost 600,000 highway bridges, many of which are deteriorated. Maintaining a reliable highway bridge system can be properly achieved via a framework that quantitatively assesses highway reliability in an accurate and computationally tractable way.

In the aftermath of natural hazards, the objectives of a reliability assessment framework are to identify the risk potentials with respect to human life and the infrastructure system; to adjust the emergency plan beforehand to reduce the potential losses and damages; to allocate the funding effectively for repair and recovery planning. In the area of the reliability analysis of transportation systems, recent methods can be grouped into two categories: qualitative and quantitative approaches. A review of qualitative approaches can be found in [4]. As an example of a qualitative approach, [5] builds a framework considering the human factor in the transportation reliability analysis and then identifies the need for both transportation systems and driving assistance systems. Recently, intelligent transportation systems (ITSs) have leveraged advanced technologies to enable effective, efficient, and safe transport [6, 7]. [8] presents the principles and selected requirements accompanying the implementation of the ITSs and the reliability and operation analysis of this type of system. [9] applies the vehicle-to-infrastructure (V2I) in the ITSs to reduce the end-to-end delay of the vehicle and improve the system reliability. [10] integrates sensor technology with the transportation infrastructure to improve road safety and traffic reliability. Among quantitative approaches, the works are either empirical surveys or

numerical simulations. [11] quantifies resilience measures of road transportation and generalizes the characteristics of the resilience response with the GPS information during severe winter storms in Wisconsin in 2008. Due to the difficulty and unavailability of data collection, the simulation-based approach is more frequently used. [12] assesses post-earthquake network damage through predictive simulation of damage states of all highway bridges. Various metrics are proposed and applied to the reliability of the transportation system, including k -terminal connectivity [13, 14, 15, 16], centrality [17, 18, 19], travel time [20, 21, 22], and resilience index [23, 24].

However, the simulation-based reliability assessments of large infrastructure networks are computationally intractable or expensive. To address this issue, [25] reduced computational complexity by using the principal component analysis (PCA) before a Monte Carlo (MC)-based uncertainty quantification. Also, surrogate techniques such as polynomial chaos expansions [26], kriging [27], and support vector machines (SVM) [28] have been proposed for network reliability analysis. Using advances in machine learning, [16] provided a deep learning framework to accelerate seismic reliability analysis of a transportation network where the k -terminal connectivity measure was used. As another example, [29] proposed a neural network surrogate for system-level seismic risk assessment of bridge transportation networks using total system travel time as the evaluation metric.

Transportation networks are expected to satisfy two requirements after an extreme event [30]: (1) maintain connectivity and desired capacity between critical origin-destination (OD) pairs immediately and (2) maintain acceptable mobility conditions for people and goods in the presence of disruptions and congestion. A rapid connectivity analysis for transportation systems is necessary to evaluate how these two requirements are satisfied. For roadway transportation systems, [16, 29] provide a graph-level evaluation including k -terminal connectivity probability and total traffic time, which is a network-level scalar measure for the whole graph. In this paper, we seek to compute a detailed node-level connectivity measure in an efficient way using a neural network-based analysis framework. Specifically, the model evaluates the connectivity probability for all origin-destination pairs after earthquakes using a graph neural network (GNN) model.

The major contributions of this work are as follows: (1) to the best of authors' knowledge, this is the first work that evaluates the connectivity for all origin-destination pairs using the graph neural network; (2) the proposed end-to-end structure of the model achieves high efficiency by avoiding extensive sampling otherwise used in Monte Carlo simulations (MCS) which reduces the computational time; and (3) the proposed model has the ability of inductive learning, i.e., it can predict node connectivities in unseen graphs. We will numerically show that the proposed framework can effectively accelerate the connectivity reliability analysis of highway bridge networks with a case study in the Bay Area in California.

The remainder of this article is structured as follows. A general simulation-based framework for connectivity analysis of transportation networks is described in Section 2. Then, Section 3 presents the node-level bridge connectivity analysis for earthquake events using a graph neural network. Furthermore, a case study of the highway bridge system in California is presented to demonstrate the accuracy and efficiency of the proposed framework in Section 4. Finally, the discussion and conclusion of the proposed framework are presented in Section 5.

2 Transportation System Reliability Analysis

A transportation network can be represented by a graph $G = (V, E)$ where V and E denote the sets of nodes and edges between these nodes, respectively. In a highway bridge system, a node is a highway intersection, and an edge is a highway segment between two intersections. Each link is denoted by $(u, v) \in E$ with u and v being the indices of its two end nodes. In this work, we assume the bridge is the only component that can fail in the network due to an earthquake, and an edge (u, v) is removed from the graph only because of a bridge failure.

Given a source node s and a target node t , s and t are connected when there exists at least one active path $l_{s,t} = \{(s, v_1), (v_1, v_2), (v_1, v_2), \dots, (v_n, t)\}$ between s and t . Let us denote the set of all possible paths as the set $L_{s,t} = \{l_{s,t}^i\}_{i=1}^{n_{s,t}}$ where $n_{s,t}$ is the total number of active path between s and t . We seek to compute the node-to-node connectivity (as a probability) using the survival probability of the bridges in the network.

To do so, we first model the survival state of the path i between s and t as a binary Bernoulli variable given by

$$x_{s,t,i} = \begin{cases} 1, & \text{with probability } p_{s,t,i}, \\ 0, & \text{with probability } 1 - p_{s,t,i}, \end{cases} \quad (1)$$

where $\{1, 0\}$ denotes the survived and failed states, respectively, with a survival probability of $p_{s,t,i}$. A path with at least one failed bridge will be removed. If path i between s and t consist of $m_{s,t,i}$ bridges, the survival probability of

the path can be represented with

$$p_{s,t,i} = \prod_{j=1}^{m_{s,t,i}} p_{s,t,i,j}, \quad (2)$$

where $p_{s,t,i,j}$ is the survival probability of the j th bridge on path i between s and t . The detail of calculating bridge survival probability is shown in Section 3.2.1.

Given bridge failure probabilities, it is however computationally intractable to directly compute the node-to-node connectivity probability from the bridge survival probability. As a result, a Monte Carlo approach is adopted, where realizations of the network are obtained by randomly removing paths based on path survival probabilities $p_{s,t,i}$ calculated using Equation 2. Specifically, for the k th MC realization of the network with the removed paths, we check all the possible paths between a given pair s and t using the breadth-first search (BFS) algorithm with time complexity of $\mathcal{O}(|\mathcal{V}| + |\mathcal{E}|)$. Then, the binary node-to-node connectivity $p_{s,t}^k$ is set equal to 1, if there is at least one path between s and t , and it is set to zero, otherwise. With N MC samples, the none-to-node connectivity probability can be approximated as

$$P_{s,t} = \frac{1}{N} \sum_{k=1}^N p_{s,t}^k. \quad (3)$$

Enough MC samples are used until the quantity of interest converges, which is set to be when the standard deviation of connectivity probability becomes less than 0.01.

3 Graph Neural Network for Node-Level Transportation System Reliability Analysis

3.1 Graph Neural Network

In most of the first applications of neural networks, e.g. in image classification, the input data is structured and typically of Euclidean structure. In graph applications, on the other hand, input is non-Euclidean and unstructured, containing different types of topologies. As such, normal neural network frameworks cannot handle graph data since the structure of the input data is not fixed. This paper leverages the graph neural network (GNN) [31] and [32] to tackle the non-Euclidean graph-structured inputs. GNN is an organic combination of connectionism and symbolism, which not only enables the deep learning model to be applicable to the non-Euclidean structure of the graph but also gives the deep learning model a certain causal reasoning ability [33].

Using the previously introduced notation for the graph, $G = (V, E)$, features used in the GNN consist of node features $X_n \subset \mathbb{R}^{|V| \times F_n}$ and edge features $X_e \subset \mathbb{R}^{|E| \times F_e}$, where $|V|$ and $|E|$ denote the number of nodes and edges, $|F_v|$ and $|F_e|$ denote the dimension of features for each node and edge. The process of combining features from a node and other nodes is called message passing. There are various approaches to exploiting node features. For instance, graph convolutional network (GCN)[34] accomplishes message passing by using the adjacency matrix A , or in an improved way by using a normalized adjacency matrix. GCN has shown great potential in many areas, for instance text classification [35], image captioning [36], and traffic prediction [37, 38].

However, the adjacency matrix contains the intra-node information, and it can only be used for transductive learning tasks, where the model is not capable of training on partial graphs and testing on unseen parts of the graph or different graphs. To overcome this obstacle, GraphSAGE [39] is proposed to enable inductive learning tasks without exploiting the adjacency matrix. This model learns to generate low-dimensional node embeddings by means of sampling and aggregating node neighbor features through the aggregation function. The widely used aggregation functions are the average operation and maximum operation [40]. GraphSAGE uses learned neural networks to aggregate information and compute the embedding based on the central vertex and its neighbors. The learned aggregation consists of two stages: feature aggregation and feature update. The learned aggregation step is modeled as a single layer in the graph neural network.

In the feature aggregation stage, at step k (or in the k^{th} layer) for each node v , we aggregate the features of its neighbors denoted by $x_u^k \in \mathbb{R}^{1 \times d_n^k}, \forall u \in \mathcal{N}(v)$ according to:

$$x_{\mathcal{N}(v)}^{k+1} = f(\{x_u^k, \forall u \in \mathcal{N}(v)\}), \forall v \in V, \quad (4)$$

where f is the aggregation function, here chosen to be the mean aggregator function, and d_n^k is the node embedding dimension at layer k . Then in the update stage at step k for each node v , the updated node features x_v^{k+1} will be computed using the previous node features $x_v^k \in \mathbb{R}^{1 \times d_n^k}$ and the aggregated features $x_{\mathcal{N}(v)}^{k+1} \in \mathbb{R}^{1 \times d_n^{k+1}}$ according to:

$$x_v^{k+1} = \sigma\left(g\left(\phi\left(x_v^k, x_{\mathcal{N}(v)}^{k+1}\right); W\right)\right), \forall v \in V, \quad (5)$$

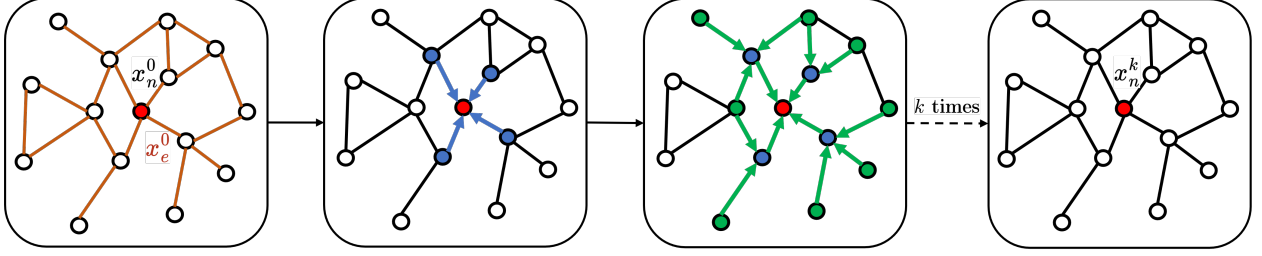


Figure 1: Message-passing with both node and edge features.

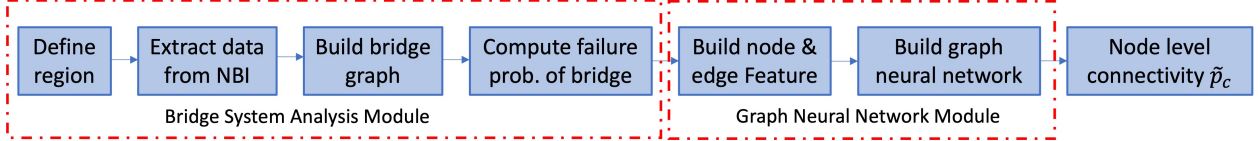


Figure 2: Pipeline of connectivity analysis of highway bridge system.

where ϕ is the concatenating function, σ is a nonlinear activation function, $g(\cdot; W)$ represents a fully connected layer with parameter W .

One weakness of GraphSAGE in the original paper [39] is that it only considers the node features and neglects the edge features. In this work, we extend the learning aggregation to include both node and edge features. At step k , edge features $x_e^k \in \mathbb{R}^{1 \times d_e^k}$ of the edge connecting each node $v, \forall v \in \mathcal{E}(v)$, are aggregated through

$$x_{\mathcal{E}(v)}^{k+1} = f(\{x_e^k, \forall e \in \mathcal{E}(v)\}), \forall v \in V. \quad (6)$$

where d_e^k is the edge embedding dimension at layer k . The aggregation step for node embedding is the same as Equation 4. Then in the update step, both node features and edge features are passed through a neural network:

$$x_v^{k+1} = \sigma\left(g\left(\phi\left(x_v^k, x_{\mathcal{N}(v)}^{k+1}, x_{\mathcal{E}(v)}^{k+1}\right); W\right)\right), \forall v \in V. \quad (7)$$

By repeatedly using Equations 4, 6 and 7, the node and edge features of multiple-hop neighbors of the central node are aggregated into the features of that central node. Figure 1 illustrates the process of message-passing when both node and edge features are passed. The left figure represents the original graph at step 0 where the node features x_n^0 and edge feature x_e^0 are initialized. Then in the aggregation step, which is shown in the middle figure, the node feature and edge feature are passed following the arrow direction. Taking the red node as an example, in step 1, the node features and edge features with blue color are passed into the red node and then updated, which are 1-hop neighbors. Then in step 2, the node features and edge features with green color are passed into the red node and then updated, which are 2-hop neighbors. After the k -step update, the node feature x_n^k includes the information from all k -hop neighbors, which is shown in the right figure. Then the node embedding can be further used for node regression and other downstream tasks.

3.2 Graph Neural Network for Bridge Connectivity Analysis

The pipeline of graph neural network surrogate for bridge connectivity analysis is shown in Figure 2. The pipeline consists of two major components: a bridge seismic analysis module and a graph neural network module.

3.2.1 Bridge Seismic Analysis Module

This module consists of generating a bridge graph and computing bridge failure probability. To generate the graph, we first need to define a region of interest for reliability analysis. The edges in the graph are highways, freeways, and expressways within the region of interest. The intersections of these roadways are considered as nodes in the graph. To calculate the bridge failure probability, the first step is to extract bridge information in the considered highway system, which could be obtained from the National Bridge Inventory (NBI)[41]. The useful information for bridge failure probability calculation includes built year, structural material, structural type, number of spans, maximum span length, bridge length, and skew angle. It should be noted that in general, an edge may consist of zero, one, or more than one bridge.

The second step for bridge failure probability calculation is to determine the ground motion at each bridge site. In this paper, the ground motion prediction equation (GMPE) is adopted, which predicts the characteristics of ground motion, including peak ground acceleration (PGA), spectral acceleration (SA), and its associated uncertainty [42, 43]. In the past decades, hundreds of GMPEs have been proposed for predicting PGA and SA. In this work, Graizer-Kalkan GMPE (GK15)[44] is adopted. The updated ground-motion prediction model for PGA has six independent predictor parameters: moment magnitude M , the closest distance to fault rupture plane in kilometers R , average shear-wave velocity in the upper 30m V_{S30} , style of faulting F , regional quality factor Q_0 , and basin depth under the site B_{depth} . In GK15, the peak ground acceleration is calculated as a multiplication of a series of functions. In the natural logarithmic scale, it is given by:

$$\ln(\text{PGA}) = \ln(G_1) + \ln(G_2) + \ln(G_3) + \ln(G_4) + \ln(G_5) + \sigma_{\ln(\text{PGA})}, \quad (8)$$

where G_1 is a scaling function for magnitude and style of faulting, G_2 models the ground-motion distance attenuation, G_3 adjusts the distance attenuation rate considering regional anelastic attenuation, G_4 models the site amplification owing to shallow site conditions, G_5 is a basin scaling function, and $\sigma_{\ln(\text{PGA})}$ represents variability in the ground motion.

In order to conduct quick assessments, rather than using the finite element analysis (FEA), the failure probability of a bridge is computed using the fragility function following the guideline of HAZUS-HM [45], developed by the Federal Emergency Management Agency (FEMA). HAZUS-HM categorizes the bridges into 28 primary types based on materials, structure type, build year, number of spans, etc. To estimate the probability of failure of bridges, the geographical location of the bridge, SA at 0.3 s and 1.0 s at the bridge location, and soil condition are also required. The form for 5% damped spectral acceleration at spectral period T is:

$$S_{a,T} = \text{PGA} \times \mu(T, M, R, V_{S30}, B_{\text{depth}}), \quad (9)$$

where μ is the spectral shape function. In HAZUS-HM, the failure probabilities of bridges are computed using the fragility curve. Five damage states are defined: none, slight, moderate, extensive, and complete damage states. For bridges, extensive damage is defined by shear failure, major settlement approach, and the vertical offset of the abutment. In this work, we assume the bridges will stop functioning when bridge damage is beyond the extensive damage state. The fragility curve for the bridge component is modeled as log-normal distribution functions characterized by median and dispersion. Furthermore, the failure probability of the j th edge on path i between s and t , $p_{s,t,i,j} \in [0, 1]$ is computed based on the assumption that the edge fails when at least one bridge fails.

3.2.2 Bridge Connectivity Analysis Module

To build the training data and testing data for graph neural networks, we need first to create node feature and edge feature using the failure probability computed in 3.2.1. The edge feature is the failure probability of each edge, which has already been computed. It should be noted that in conventional connectivity analysis there is no feature directly assigned to the nodes, i.e. intersection of the roadways. In this work, however, we consider node features in the graph neural network models. Four local and global graph characteristics are considered as features of node v : the degree of the node $\text{deg}(v)$; the largest failure probability of edges connected to the node $\max(\{p(e), \forall e \in \mathcal{E}(v)\})$; the smallest failure probability of edges connected to the node $\min(\{p(e), \forall e \in \mathcal{E}(v)\})$ and number of hops on the shortest path to the target node t $h(v, t)$. All the node features in the graph are denoted by $X_n \in \mathbb{R}^{|N| \times F_n}$ with the number of node feature $F_n = 4$.

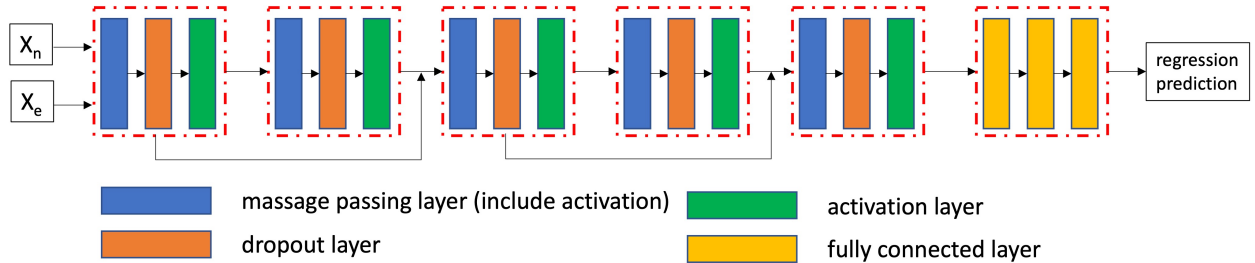


Figure 3: Architecture of graph neural network model for node-level connectivity analysis.

The proposed node features characterize each node from several perspectives: the degree represents the possible paths connecting the node to its neighbors; the range of failure probabilities of edges connected to the node represents the

Table 1: Statistic of different region levels

Graph Level	# Node N_n	# Edge N_e	# Bridge N_b
Level 1	39	64	245
Level 2	84	133	448
Level 3	103	159	628

distribution of the failure probability; the number of hops represents a global feature characterizing the distance with respect to the target node. It should be noted that in addition to the range of edge failure probabilities (i.e. the largest and smallest failure probabilities of connected edges), one can also consider multiple quantiles to more precisely capture the distribution of failure probabilities for a potentially more accurate analysis.

Another difficulty in the graph neural network is the over-smoothing issue. In particular, because of the aggregation and update operations in the message passing, the interacting nodes have similar representations and the feature embeddings of different nodes in the deep graph neural network would tend to be similar. To alleviate this issue, differentiable group normalization [46] and dropEdge[47] were proposed to add normalization into graph neural networks in different forms. In this work, we add a dropout layer after the message-passing layer since dropout can randomly remove neurons in the forward propagation. It is equivalent to randomly removing edge features and node features from the original graph in the training process, which can be considered as a normalization strategy.

The architecture of the proposed graph neural network model for bridge connectivity analysis is shown in Figure 3. A single block of message passing consists of a message passing layer, a dropout layer, and an activation layer. The skipping layer connection is used in our proposed architecture to mitigate vanishing or exploding gradient problems. A regression block with multiple feed-forward fully connected layers is concatenated after the last message passing block. The output of the model is the node-level connectivity probability $P_c \in \mathbb{R}^{|V| \times 1}$. The L1 loss is used for quantifying the difference between the MCS and prediction.

4 Experiments and Results

4.1 Experiment Setup

The proposed GNN-based reliability analysis is applied to the highway bridge system of the California Bay Area. The transportation system contains highways, freeways, and expressways connecting major airports and hospitals. The considered study area includes the major cities of Santa Clara, Mountain View, and San Jose, with a large population base. Therefore, it is important to maintain the connectivity of the highway bridge system after extreme events. In this experiment, three different regions of study are considered (levels 1 to 3). The map illustrations are shown in Figure 4 obtained from Google Map [48]. The characteristics of these three regions, specifically their number of nodes, N_n , number of edges, N_e , and number of bridges, N_b , are shown in Table 1.

The 1989 Loma Prieta earthquake is chosen as the seismic event. The earthquake is scaled to different magnitudes, M , in the range between 6.5 and 8.0. To generate the training data, the earthquake magnitude M_i is sampled from

$$M_i = M_u - \lambda_i, \quad (10)$$

Where M_u is the upper bound of the possible earthquake magnitude and set to be 8.0 in this study, and λ_i is a random sample following truncated exponential distribution with the shape parameter of 1.5. Figure 2 shows the pipeline of data generation. In the Monte Carlo simulation (MCS) approach, the number of samples N_s is set to 10,000. For each node in the graph, N_k earthquake realizations are generated, and in total, $N_k \times N_n$ network realizations are generated.

The graph neural network used in this work consists of five graph message passing layers and three fully connected layers for regression purposes. The dimension of the hidden message passing layer and fully connected layer is 64. The rectified linear unit (ReLU) is chosen as the activation function. The dropout rate is set to 0.1, and the Adam optimizer is used to minimize the L1 loss, which is the mean absolute error, with a learning rate of 0.001. The model is trained using mini-batch training with 200 epochs and a batch size of 64.

For the train-test split, we first held out 20% of the nodes for testing. To ensure that the removed nodes are more or less evenly scattered on the network, one can partition the graph and select a number of nodes from each partition. However, uniform graph partitioning or a balanced graph partition problem can be shown to be NP-complete. As the problem size increases, the time to find the optimal solution increases exponentially [49]. As a result, the serial graph partitioning

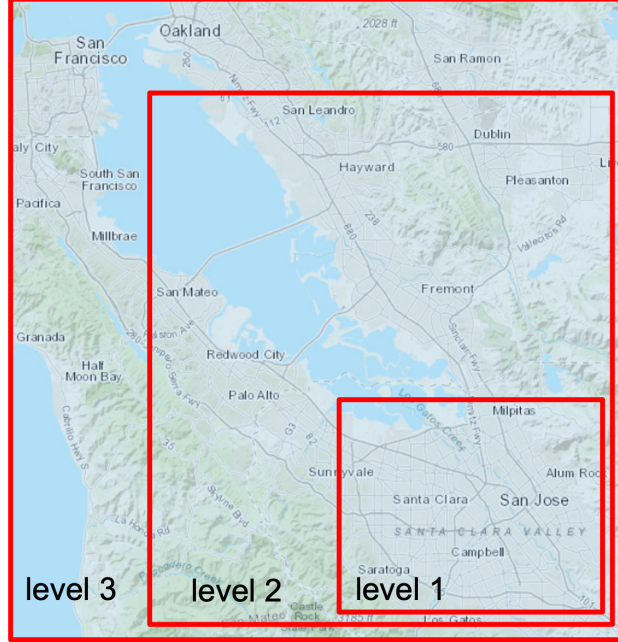


Figure 4: Map illustration of the studied regions in different levels [48].

algorithm [50] is applied for approximately partitioning of the graph. Then we determine the percentage of training nodes to determine the number of nodes used for training and the training node is selected from each partitioned graph.

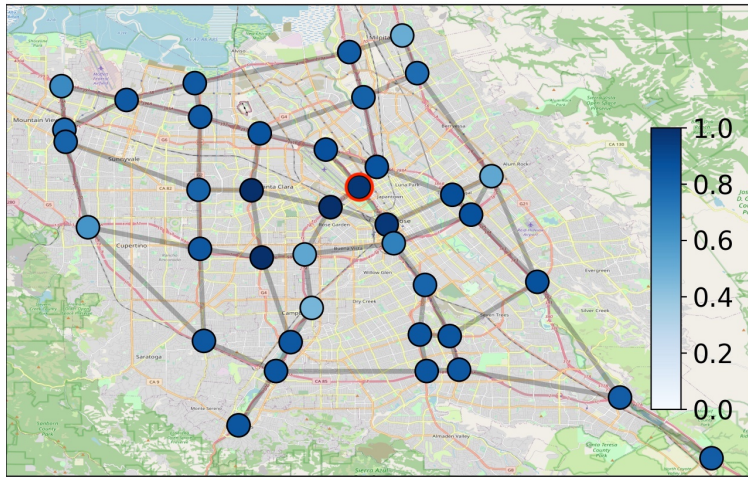
4.2 Prediction Results

We test the performance of the proposed approach from multiple perspectives. First, we consider a regression problem where we calculate the probability of connectivity between a target node and the rest of the nodes in the region. The target node is located in downtown San Jose, which is a critical location for the large population base. We do this for three regions of interest. The prediction results for the Level 1 region are shown in Figure 5. The mean absolute error (MAE) between Monte Carlo simulation (MCS) and GNN predictions was calculated. The maximum MAE in the graph is 0.032 and the average MAE is 0.013. This demonstrates the accuracy of the proposed GNN surrogate model. Figure 6 shows the prediction results and the corresponding error for the Level 3 graph. For this case, the maximum MAE in the graph is 0.055 and the mean prediction MAE is 0.019.

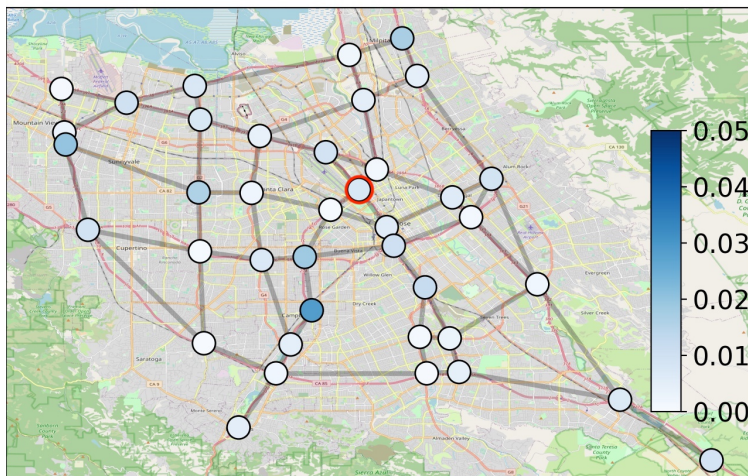
Furthermore, from the perspective of decision-making, the actual node connectivity probability may not be needed. Instead, stakeholders may choose to consider a set of node connectivity classes. In this case, we evaluate how accurate the predicted classes will be compared to the MCS approach. It should be noted that a different classification model is not trained in this case. We only predict the connectivity classes by assigning the predicted connectivity probability of each node into a class. In this example, three classes for node connectivity probabilities, namely normal connection, minor disconnection and major disconnection, for the connectivity probabilities falling in the ranges $[0.75, 1.0]$, $[0.5, 0.75]$ and $[0, 0.5]$, respectively. The node connectivity conditions are directly classified based on the connectivity probability from the regression result. Figure 7 shows the classification result using the same example in Figure 5. F1 score is chosen as the classification evaluation metric F1 score, which is 1.0 in this example.

In order to assess the robustness of the proposed approach, we run several experiments in which the number of training nodes within the graph varies. Specifically, a subset of the nodes is considered as the target nodes in training. In all the experiments, 20% of the nodes in the graph are selected as the "test" target nodes, which are made sure to be different from the "training" target nodes. For each case, a specific ratio of the graph nodes is selected as the "training" target nodes. These ratios are chosen between 5% and 80%. The evaluation metrics include mean square error, mean absolute error, and F1 score. The performances with different levels are demonstrated in Figure 8, which shows that when the ratio of training target nodes is from 20% to 40%, the F1 score can reach 0.85 and MAE is less than 0.08. Furthermore, when the training target node ratio is 60%, the F1 score can reach above 0.9, and MAE is less than 0.01.

To further evaluate the robustness of the proposed approach, Figure 9 compares the MCS and GNN predictions of node connectivity for all earthquake realizations. The percentage in each figure indicates the ratio of false positive (FP) and



(a) Predicted connectivity probability from GNN

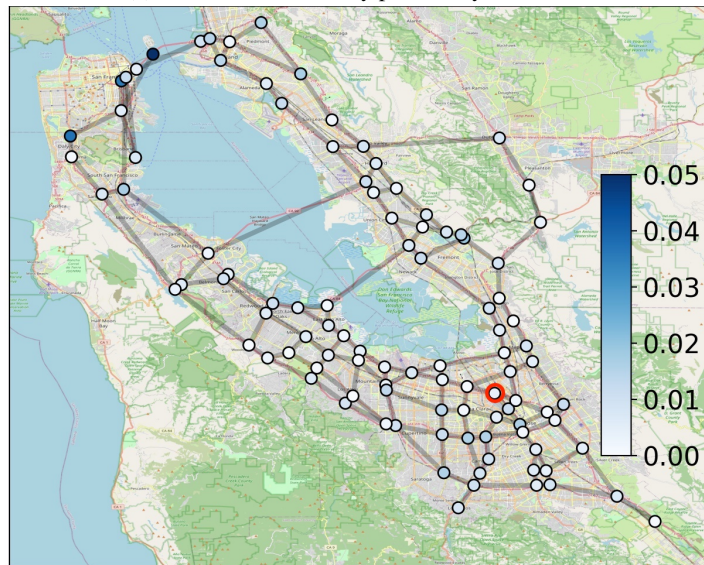


(b) Absolute error between GNN and MCS predictions

Figure 5: Prediction of connectivity probabilities between the target node (red circle) and the other nodes in the Level 1 region. The nodes are color-coded based on the predicted connectivity probability (top) and the absolute error between predicted connectivity probabilities from GNN and MCS (bottom).

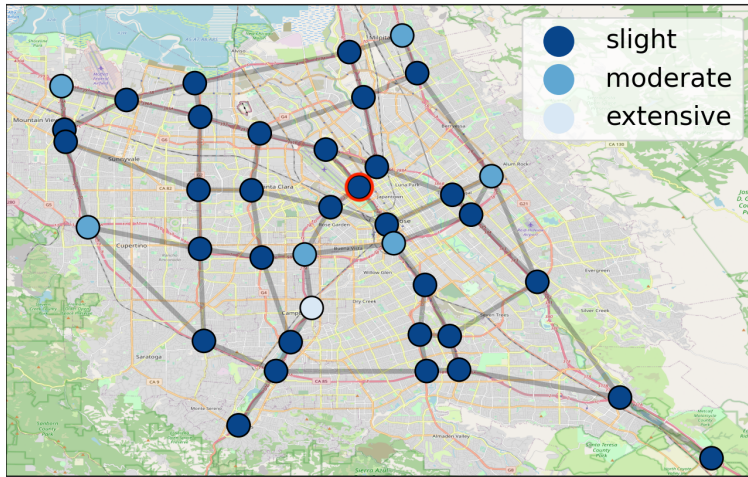


(a) Predicted connectivity probability from GNN

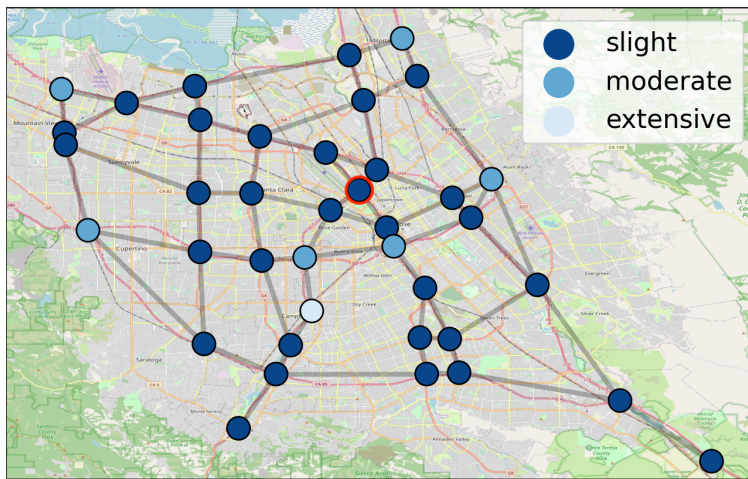


(b) Absolute error between MCS and GNN predictions

Figure 6: Prediction of connectivity probabilities between the target node (red circle) and the other nodes in the Level 3 region. The nodes are color-coded based on the predicted connectivity probability (top) and the absolute error between predicted connectivity probabilities from GNN and MCS (bottom).



(a) Predicted connectivity classes from MCS



(b) Predicted connectivity class from GNN

Figure 7: Identical predictions of connectivity classes obtained from GNN and MCS models for the Level 1 region. The red circle shows the target node. Three classes represent normal connection, minor disconnection, and major disconnection.

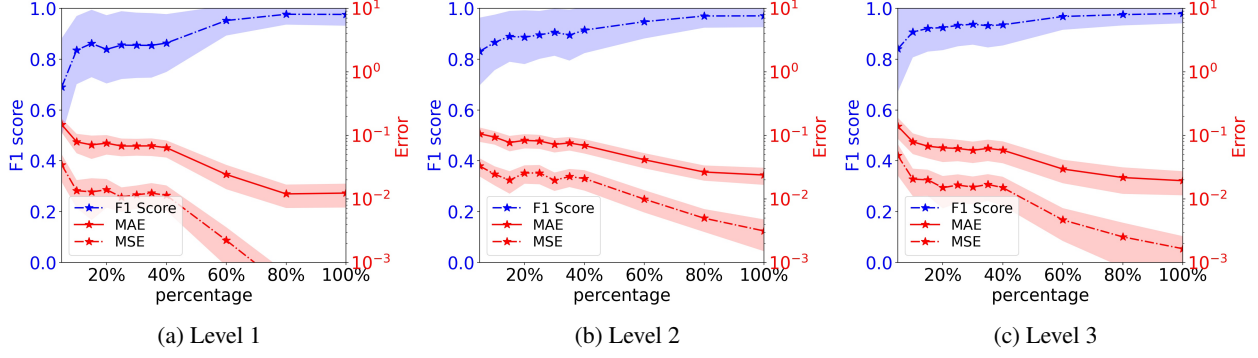


Figure 8: Relationship between different metrics and the percentage of training nodes shown for the three regions.

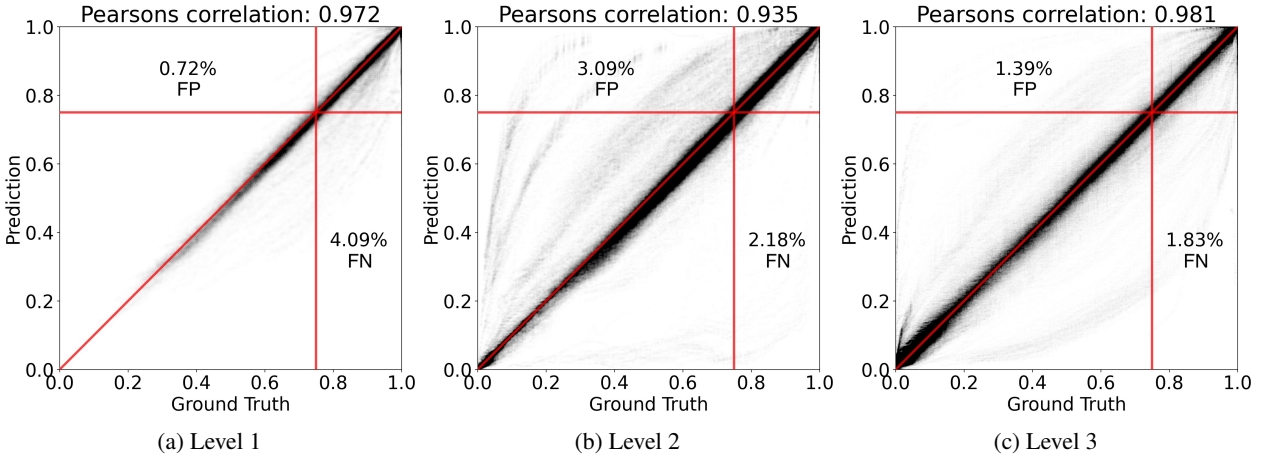


Figure 9: Relationship between predicted node connectivity and MCS predictions shown for the three regions. The percentage in the figure represents the proportion of false positive (FP) and false negative (FN) results.

false negative (FN) samples among all samples with the cutoff threshold 0.75, which is less than 5%. It can also be seen that the Pearson Correlation coefficients between MCS and GNN prediction for all region levels are higher than 0.93. Table 2 summarizes the performance metrics and the computational times for different regions. The F1 scores are calculated for two cases, where the predicted connectivity probability is turned into one of two classes, [0-0.5] or [0.5-1], or into one of the three aforementioned classes. The computational time for the proposed GNN model considers both training time and inference time, and as can be seen is 20× shorter than that of MCS.

4.3 Model Performance Under Special Cases

Neural networks are vulnerable to adversarial examples and [51, 52], where a small perturbation to the original data will change the neural network prediction drastically. To illustrate the robustness of our approach in these cases, the proposed GNN model is evaluated on the slightly modified testing data. As the context, we consider the cases where

Table 2: Comparison between performance metrics and computational times between GNN and MCS, averaged over 100 experiments for each region. The cutoff thresholds for two-class and three-class classification are {0.5} and {0.5, 0.75}, respectively.

Graph Level	MAE	MSE	F1 score (2 class)	F1 score (3 class)	Time (GNN)	Time (MC)
Level 1	0.012	0.001	0.947	0.935	4.7 min	118.2 min
Level 2	0.025	0.008	0.952	0.906	13.6 min	490.3 min
Level 3	0.013	0.002	0.972	0.942	29.6 min	698.2 min

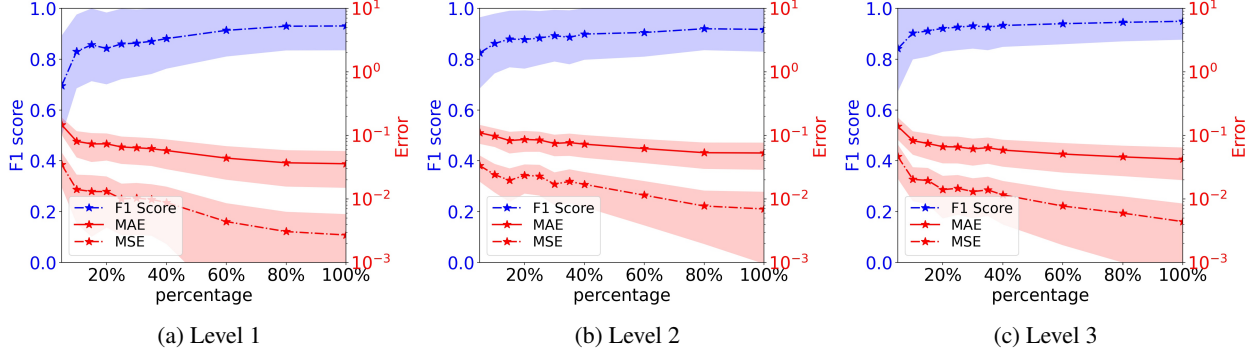


Figure 10: Relationship between different performance metrics and different ratios of training target nodes, shown for the three regions with perturbed edge features.

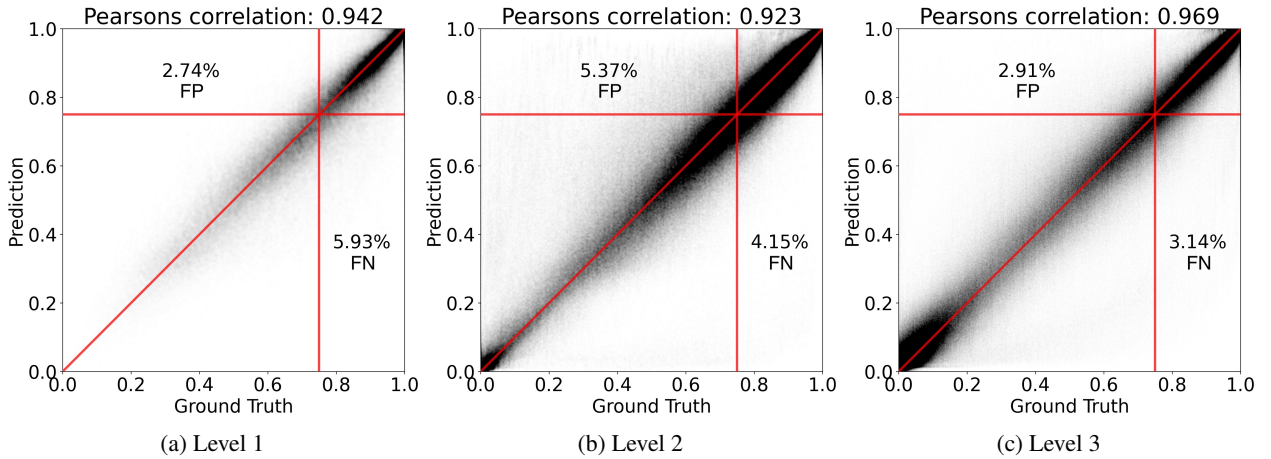


Figure 11: Comparison of predicted node connectivity between MCS and GNN in the three regions with perturbed edge features.

bridge failure probabilities are decreased or increased because of repairs or deterioration through the life cycle. To test the robustness of the proposed model among all region levels, we generate perturbed features by adding to each edge failure probability a zero-mean Gaussian noise with a standard deviation set equal to 20% of the original edge failure probability. The resulting failure probability is truncated at 0 and 1. Following this perturbation to the edge features, the node features are also updated accordingly. Then the GNN prediction of node connectivities is performed for all three regions as described in Section 4.2 and the comparison between the prediction and MCS in this perturbed case is also shown in Figures 10 and 11. It can be seen in Figure 11, that even though there is more discrepancy between the GNN and MCS compared to the original case in Figure 9, overall the performance is acceptable for an unseen case where all edges have different features. The F1 score of prediction with perturbed data is 0.958, 0.949, and 0.961 for three region levels respectively. The correlation coefficient of prediction with perturbed data is 0.942, 0.923, and 0.969 for three region levels respectively.

Finally, we assess the capability of the proposed approach in generalization or *inductive* inference and prediction. Specifically, we evaluate whether the model can be used for predicting out-of-distribution (OOD) data, that is, producing accurate predictions for test cases that are distributed differently from the way training data was distributed. As opposed to transfer learning where the model is retrained on the new data, in generalization or inductive learning, we do not modify the previously trained model and only evaluate it on the new data. In practice, this can be used to assess the network connectivity when new bridges or roads are either added in a network expansion or removed due to a disaster.

In these cases, to assess whether the trained model has generalization capacity without additional fine-tuning, we consider the base training of the model to be done at the Level 2 region level. We then test the performance of the trained model on the Level 3 region. In general, this is a challenging task because many of the nodes in the larger Level 3 region are unseen and were not included in the previous training. However, as can be seen in Figure 12, the proposed GNN model has an acceptable performance. It can be seen that the F1 score in this case is 0.92 even though only 60%

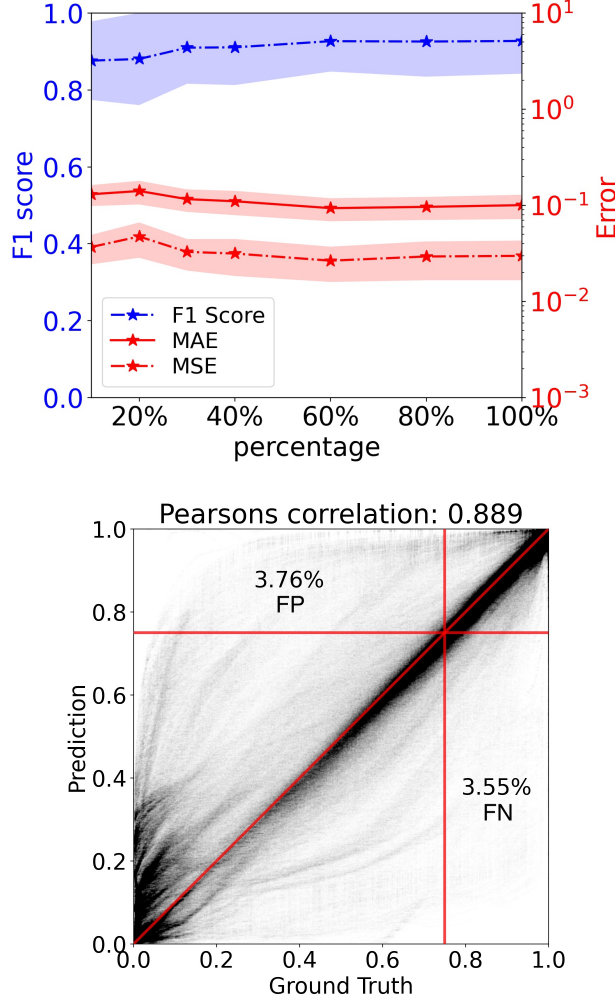


Figure 12: Assessment of the performance of inductive learning from the smaller Level 2 region to Level 3 region, in terms of the classification results (top) and regression results (bottom).

of the nodes in the smaller region (Level 2) were used as training nodes, for a prediction at a large region (Level 3). This good performance in handling inductive learning tasks is achieved because the mechanism of the message passing used in the GNN architecture enables a modular understanding of how the graph features are aggregated and collectively influence the task at hand.

5 Conclusion and Discussion

Rapid evaluation of large-scale infrastructure system reliability is critical to enhance the preparation, risk mitigation and response management under probabilistic natural hazard events. In this paper, we propose a rapid seismic reliability assessment approach for roadway transportation systems with seismic damage on bridges using the graph neural network. Compared with the common reliability assessment approaches, which consider the response at the system or graph level, we focus on a more detailed notion of reliability where the seismic impact is quantified at the node-level for transportation systems. The proposed GNN surrogate bypasses extensive sampling that is required in Monte Carlo-based approaches and offers high efficiency while preserving the accuracy. Additionally, the message passing component of the proposed GNN model creates a modular model structure which can offer a good generalization capacity, i.e., can effectively predict system reliability in unseen graphs. The numerical experiments in this work, carried out on a transportation system in California, demonstrate the effectiveness, robustness, and efficiency of the proposed approach in enabling rapid assessment of large-scale network reliability with high accuracy. As extensions to this work, measures other than node-to-node connectivity can be considered. Examples include travel distance, travel time, or traffic flow.

Another area for future research is the investigation of an efficient optimization framework based on the proposed GNN approach for selecting the best maintenance planning strategy.

References

- [1] Jamie Padgett, Reginald DesRoches, Bryant Nielson, Mark Yashinsky, Oh-Sung Kwon, Nick Burdette, and Ed Tavera. Bridge damage and repair costs from hurricane katrina. *Journal of Bridge Engineering*, 13(1):6–14, 2008.
- [2] Caiyu Sun and Jiuping Xu. Estimation of time for wenchuan earthquake reconstruction in china. *Journal of Construction Engineering and Management*, 137(3):179–187, 2011.
- [3] Critical infrastructure sectors, 2022.
- [4] Chengpeng Wan, Zaili Yang, Di Zhang, Xiping Yan, and Shiqi Fan. Resilience in transportation systems: a systematic review and future directions. *Transport Reviews*, 38(4):479–498, Jul 2018.
- [5] Subeer Rangra, Mohamed Sallak, Walter Schön, and Frédéric Vanderhaegen. On the study of human reliability in transportation systems of systems. In *2015 10th System of Systems Engineering Conference (SoSE)*, pages 208–213. IEEE, 2015.
- [6] Li Zhu, Fei Richard Yu, Yige Wang, Bin Ning, and Tao Tang. Big data analytics in intelligent transportation systems: A survey. *IEEE Transactions on Intelligent Transportation Systems*, 20(1):383–398, 2018.
- [7] Agachai Sumalee and Hung Wai Ho. Smarter and more connected: Future intelligent transportation system. *Iatss Research*, 42(2):67–71, 2018.
- [8] Mirosław Siergiejczyk, Karolina Krzykowska, Adam Rosinski, and Luigi Alfredo Grieco. Reliability and viewpoints of selected its system. In *2017 25th International Conference on Systems Engineering (ICSEng)*, pages 141–146. IEEE, 2017.
- [9] Hong Zhang and Xinxin Lu. Vehicle communication network in intelligent transportation system based on internet of things. *Computer Communications*, 160:799–806, 2020.
- [10] Juan Guerrero-Ibáñez, Sherali Zeadally, and Juan Contreras-Castillo. Sensor technologies for intelligent transportation systems. *Sensors*, 18(4):1212, 2018.
- [11] Teresa M Adams, Kaushik R Bekkem, and Edwin J Toledo-Durán. Freight resilience measures. *Journal of Transportation Engineering*, 138(11):1403–1409, 2012.
- [12] S Banerjee and M Shinozuka. Uncertainties in seismic risk assessment of highway transportation systems. In *TCLÉE 2009: Lifeline Earthquake Engineering in a Multihazard Environment*, pages 1–9. 2009.
- [13] Benny Sudakov and Van H Vu. Local resilience of graphs. *Random Structures & Algorithms*, 33(4):409–433, 2008.
- [14] Sybil Derrible and Christopher Kennedy. The complexity and robustness of metro networks. *Physica A: Statistical Mechanics and its Applications*, 389(17):3678–3691, 2010.
- [15] Xiaodong Zhang, Elise Miller-Hooks, and Kevin Denny. Assessing the role of network topology in transportation network resilience. *Journal of transport geography*, 46:35–45, 2015.
- [16] Mohammad Amin Nabian and Hadi Meidani. Deep learning for accelerated seismic reliability analysis of transportation networks. *Computer-Aided Civil and Infrastructure Engineering*, 33(6):443–458, 2018.
- [17] Yew-Yih Cheng, Roy Ka-Wei Lee, Ee-Peng Lim, and Feida Zhu. Measuring centralities for transportation networks beyond structures. In *Applications of social media and social network analysis*, pages 23–39. Springer, 2015.
- [18] Andrew Cook, Henk AP Blom, Fabrizio Lillo, Rosario Nunzio Mantegna, Salvatore Micciche, Damián Rivas, Rafael Vázquez, and Massimiliano Zanin. Applying complexity science to air traffic management. *Journal of Air Transport Management*, 42:149–158, 2015.
- [19] Ralihalizara Julliard, PJ Yun, and Ranaivoson Rado. Robustness of transportation networks: The case of madagascar’s road network. *International Journal of Advancements in Research & Technology*, 4(5):1–4, 2015.
- [20] Mayada Omer, Ali Mostashari, and Roshanak Nilchiani. Measuring the resiliency of the manhattan points of entry in the face of severe disruption. *American Journal of Engineering and Applied Sciences*, 4(1):153–161, 2011.

- [21] Reigna Jewel Ritz Meman Macababba and Jose Regin Fajardo Regidor. A study on travel time and delay survey and traffic data analysis and visualization methodology. In *Proceedings of the Eastern Asia Society for Transportation Studies Vol. 8 (The 9th International Conference of Eastern Asia Society for Transportation Studies, 2011)*, pages 318–318. Eastern Asia Society for Transportation Studies, 2011.
- [22] Pavithra Parthasarathi, David Levinson, and Hartwig Hochmair. Network structure and travel time perception. *PloS one*, 8(10):e77718, 2013.
- [23] Aman Karamlou and Paolo Bocchini. From component damage to system-level probabilistic restoration functions for a damaged bridge. *Journal of Infrastructure Systems*, 23(3):04016042, 2017.
- [24] A Karamlou, P Bocchini, and V Christou. Metrics and algorithm for optimal retrofit strategy of resilient transportation networks. *Maintenance, monitoring, safety, risk and resilience of bridges and bridge networks*, pages 1121–1128, 2016.
- [25] Mohammad Amin Nabian and Hadi Meidani. Uncertainty quantification and pca-based model reduction for parallel monte carlo analysis of infrastructure system reliability. In *96th Annual Meeting of the Transportation Research Board, Washington DC*, 2017.
- [26] Nestor V Queipo, Raphael T Haftka, Wei Shyy, Tushar Goel, Rajkumar Vaidyanathan, and P Kevin Tucker. Surrogate-based analysis and optimization. *Progress in aerospace sciences*, 41(1):1–28, 2005.
- [27] Vincent Dubourg, Bruno Sudret, and Jean-Marc Bourinet. Reliability-based design optimization using kriging surrogates and subset simulation. *Structural and Multidisciplinary Optimization*, 44(5):673–690, 2011.
- [28] Raphael E Stern, Junho Song, and Daniel B Work. Accelerated monte carlo system reliability analysis through machine-learning-based surrogate models of network connectivity. *Reliability Engineering & System Safety*, 164:1–9, 2017.
- [29] Sungsik Yoon, Jeongseob Kim, Minsun Kim, Hye-Young Tak, and Young-Joo Lee. Accelerated system-level seismic risk assessment of bridge transportation networks through artificial neural network-based surrogate model. *Applied Sciences*, 10(18):6476, 2020.
- [30] Yafeng Yin and Hitoshi Ieda. Assessing performance reliability of road networks under nonrecurrent congestion. *Transportation Research Record*, 1771(1):148–155, 2001.
- [31] Alessandro Sperduti and Antonina Starita. Supervised neural networks for the classification of structures. *IEEE Transactions on Neural Networks*, 8(3):714–735, 1997.
- [32] Marco Gori, Gabriele Monfardini, and Franco Scarselli. A new model for learning in graph domains. In *Proceedings. 2005 IEEE international joint conference on neural networks*, volume 2, pages 729–734, 2005.
- [33] Jie Zhou, Ganqu Cui, Shengding Hu, Zhengyan Zhang, Cheng Yang, Zhiyuan Liu, Lifeng Wang, Changcheng Li, and Maosong Sun. Graph Neural Networks: A Review of Methods and Applications. *arXiv*, Dec 2018.
- [34] Thomas N. Kipf and Max Welling. Semi-Supervised Classification with Graph Convolutional Networks. *arXiv*, Sep 2016.
- [35] Liang Yao, Chengsheng Mao, and Yuan Luo. Graph convolutional networks for text classification. In *Proceedings of the AAAI conference on artificial intelligence*, volume 33, pages 7370–7377, 2019.
- [36] Ting Yao, Yingwei Pan, Yehao Li, and Tao Mei. Exploring visual relationship for image captioning. In *Proceedings of the European conference on computer vision (ECCV)*, pages 684–699, 2018.
- [37] Yaguang Li, Rose Yu, Cyrus Shahabi, and Yan Liu. Diffusion Convolutional Recurrent Neural Network: Data-Driven Traffic Forecasting. *arXiv*, Jul 2017.
- [38] Tanwi Mallick, Prasanna Balaprakash, Eric Rask, and Jane Macfarlane. Graph-partitioning-based diffusion convolutional recurrent neural network for large-scale traffic forecasting. *Transp. Res. Rec.*, 2674(9):473–488, Jul 2020.
- [39] William L Hamilton, Rex Ying, and Jure Leskovec. Inductive representation learning on large graphs. In *Proceedings of the 31st International Conference on Neural Information Processing Systems*, pages 1025–1035, 2017.
- [40] Simon Geisler, Daniel Zügner, and Stephan Günnemann. Reliable graph neural networks via robust aggregation. *Advances in Neural Information Processing Systems*, 33:13272–13284, 2020.
- [41] National bridge inventory, 2018.
- [42] Jonathan P Stewart, John Douglas, Mohammad Javanbarg, Yousef Bozorgnia, Norman A Abrahamson, David M Boore, Kenneth W Campbell, Elise Delavaud, Mustafa Erdik, and Peter J Stafford. Selection of ground motion prediction equations for the global earthquake model. *Earthquake Spectra*, 31(1):19–45, 2015.

- [43] Julian J Bommer, John Douglas, Frank Scherbaum, Fabrice Cotton, Hilmar Bungum, and Donat Fah. On the selection of ground-motion prediction equations for seismic hazard analysis. *Seismological Research Letters*, 81(5):783–793, 2010.
- [44] Vladimir Graizer and Erol Kalkan. Summary of the GK15 Ground-Motion Prediction Equation for Horizontal PGA and 5% Damped PSA from Shallow Crustal Continental Earthquakes Summary of the GK15 GMPE for Horizontal PGA and 5% Damped PSA. *Bull. Seismol. Soc. Am.*, 106(2):687–707, Apr 2016.
- [45] FEMA. *HAZUS-MH MR5 Technical Manual - Earthquake Model*. U.S. Department of Homeland Security, 2010.
- [46] Kaixiong Zhou, Xiao Huang, Yuening Li, Daochen Zha, Rui Chen, and Xia Hu. Towards deeper graph neural networks with differentiable group normalization. *arXiv preprint arXiv:2006.06972*, 2020.
- [47] Yu Rong, Wenbing Huang, Tingyang Xu, and Junzhou Huang. Dropedge: Towards deep graph convolutional networks on node classification. *arXiv preprint arXiv:1907.10903*, 2019.
- [48] Google. Google map, 2022.
- [49] Tomas Feder, Pavol Hell, Sulamita Klein, and Rajeev Motwani. Complexity of graph partition problems. In *Proceedings of the thirty-first annual ACM symposium on Theory of computing*, pages 464–472, 1999.
- [50] George Karypis and Vipin Kumar. MeTis: Unstructured Graph Partitioning and Sparse Matrix Ordering System, Version 4.0, 2022.
- [51] Xiaowei Huang, Daniel Kroening, Wenjie Ruan, James Sharp, Youcheng Sun, Emese Thamo, Min Wu, and Xinping Yi. A survey of safety and trustworthiness of deep neural networks: Verification, testing, adversarial attack and defence, and interpretability. *Computer Science Review*, 37:100270, 2020.
- [52] Han Xu, Yao Ma, Hao-Chen Liu, Debayan Deb, Hui Liu, Ji-Liang Tang, and Anil K Jain. Adversarial attacks and defenses in images, graphs and text: A review. *International Journal of Automation and Computing*, 17(2):151–178, 2020.